

DOI:10.1002/ejic.201500161

# Comparative Study of the Reactivity of Zirconium(IV)-Substituted Polyoxometalates towards the Hydrolysis of Oligopeptides

Hong Giang T. Ly,<sup>[a]</sup> Gregory Absillis,<sup>[a]</sup> and Tatjana N. Parac-Vogt\*<sup>[a]</sup>

**Keywords:** Enzyme mimics / Peptidases / Oligopeptides / Polyoxometalates / Hydrolysis / Zirconium

The hydrolytic activity of the Zr<sup>IV</sup>-substituted Keggin-type (Et<sub>2</sub>NH<sub>2</sub>)<sub>8</sub>[( $\mu$ -PW<sub>11</sub>O<sub>39</sub>Zr-( $\mu$ -OH)(H<sub>2</sub>O))<sub>2</sub>] $\cdot$ 7H<sub>2</sub>O (**1**), Lindqvist-type (Me<sub>4</sub>N)<sub>2</sub>[W<sub>5</sub>O<sub>18</sub>Zr(H<sub>2</sub>O)<sub>3</sub>] (**2**), and Wells–Dawson-type Na<sub>14</sub>[Zr<sub>4</sub>(P<sub>2</sub>W<sub>16</sub>O<sub>59</sub>)<sub>2</sub>( $\mu_3$ -O)<sub>2</sub>(OH)<sub>2</sub>(H<sub>2</sub>O)<sub>4</sub>] $\cdot$ 57H<sub>2</sub>O (**3**) polyoxometalates (POMs) towards the peptide bonds in the oligopeptides triglycine, tetraglycine, glycylglycylhistidine, and glycylserylphenylalanine was investigated by kinetic methods and multinuclear NMR spectroscopy. <sup>31</sup>P NMR and UV/Vis spectroscopy showed that **1–3** were stable under the conditions used to study peptide bond hydrolysis. The reactivity of **1–3** towards oligopeptides was compared on the basis of the amount of free glycine produced at a certain time increment. In the presence of **1–3**, rate constants in the range

6.25  $\times$  10<sup>-7</sup> to 10.14  $\times$  10<sup>-7</sup> s<sup>-1</sup> were obtained, whereas no hydrolysis was observed after one month in the absence of these POMs. The results showed that the Keggin-type complex **1** was the most active towards peptide bond hydrolysis in tri- and tetrapeptides. <sup>1</sup>H and <sup>13</sup>C NMR spectroscopy showed that triglycine, tetraglycine, and glycylserylphenylalanine interact with **1** and **2** preferentially through the amine nitrogen atom and the N-terminal amide oxygen atom to activate the peptide bond towards hydrolysis. The coordination of glycylglycylhistidine resulted in multiple complexes with **1–3** as a result of additional imidazole coordination to the Zr<sup>IV</sup> centers.

## Introduction

Polyoxometalates (POMs) are composed of Mo<sup>VI</sup>, W<sup>VI</sup>, and/or V<sup>V</sup> ions bridged by oxo ligands.<sup>[1]</sup> Under appropriate reaction conditions, they undergo hydrolysis to form lacunary structures that can act as ligands for metal ions and, thereby, forming metal-substituted POMs (MSPs). A broad range of transition-metal and lanthanide ions have already been incorporated into lacunary POM species of the Lindqvist, Keggin, and Wells–Dawson types.<sup>[2]</sup> Owing to their structural diversity and their highly tunable physical and chemical properties, MSPs have attracted considerable attention in the fields of catalysis, medicine, and materials science.<sup>[2b,3]</sup> MSPs are particularly interesting for catalysis applications owing to the Lewis acidity or redox properties of the embedded metal centers and the charged surface of the POM, which can interact with the substrate through electrostatic, van der Waals, or hydrogen-bond interactions.<sup>[3d,3f,4]</sup> For example, MSPs have been developed as effective catalysts for H<sub>2</sub>O<sub>2</sub>- and O<sub>2</sub>-based green oxidations. The MSP-catalyzed epoxidations of various substrates such as olefins, allylic, and homoallylic alcohols as well as the

oxidations of various sulfides in the presence of H<sub>2</sub>O<sub>2</sub> have been reported.<sup>[5]</sup> Moreover, the application of MSPs as effective homogeneous catalysts for water oxidation has also been demonstrated recently.<sup>[6]</sup> MSPs also act as Lewis acid catalysts for esterification and C–C bond formation in Mannich, Diels–Alder, and Mukaiyama reactions.<sup>[7]</sup> The catalytic activities of Hf<sup>IV</sup>- and Zr<sup>IV</sup>-substituted Keggin- and Wells–Dawson-type POMs such as [ $\alpha_1$ -M(OH)-PW<sub>11</sub>O<sub>39</sub>]<sup>4-</sup> and [ $\alpha_1$ -M(H<sub>2</sub>O)<sub>4</sub>P<sub>2</sub>W<sub>17</sub>O<sub>61</sub>]<sup>6-</sup> are higher than those of their lanthanide analogs as a result of the increased Lewis acidity of the Hf<sup>IV</sup> and Zr<sup>IV</sup> centers.<sup>[7c,7d]</sup>

Interestingly, Hf<sup>IV</sup>- and Zr<sup>IV</sup>-substituted POMs also act as efficient catalysts for both phosphoester and peptide bond hydrolysis in dipeptides and proteins such as hen egg white lysozyme, human serum albumin, and bovine serum albumin.<sup>[8]</sup> Unactivated peptide bonds are extremely stable under physiological conditions, and the estimated half-life for their hydrolysis is up to 600 years.<sup>[9]</sup> As peptides are effective ligands for metal ions under physiological conditions owing to their high metal binding affinity,<sup>[10]</sup> many transition-metal or lanthanide ions and their complexes have emerged as promising reagents for the hydrolysis of peptides and proteins.<sup>[11]</sup> Reactivity towards peptide bond hydrolysis was observed in the presence of Ce<sup>IV</sup>, Zr<sup>IV</sup>, and Hf<sup>IV</sup> complexes owing to the strong Lewis acidic and oxophilic nature of these metal ions as well as the high coordination numbers and flexible coordination geometries of

[a] Department of Chemistry, KU Leuven, Celestijnenlaan 200F, 3001 Leuven, Belgium  
E-mail: Tatjana.Vogt@chem.kuleuven.be  
<http://chem.kuleuven.be/lbc/>

Supporting information for this article is available on the WWW under <http://dx.doi.org/10.1002/ejic.201500161>.

the resulting complexes.<sup>[11]</sup> Therefore, in our quest to further develop MSPs as Lewis acid catalysts for peptide bond hydrolysis, we recently focused our attention on Zr<sup>IV</sup>-substituted POMs.

The sandwich 1:2 Zr<sup>IV</sup>-substituted Wells–Dawson POM was the first POM that exhibited peptide bond hydrolysis in a variety of dipeptides and oligopeptides under mildly acidic conditions.<sup>[8b,8f,8g,12]</sup> Their hydrolysis was significantly accelerated owing to the binding of the Zr<sup>IV</sup> ion to the amine nitrogen atom and the amide carbonyl oxygen atom. Lewis acid mediated dipeptide hydrolysis by the dimeric dizirconium(IV)-substituted Keggin POM (Et<sub>2</sub>NH<sub>2</sub>)<sub>8</sub>[{ $\alpha$ -PW<sub>11</sub>O<sub>39</sub>Zr-( $\mu$ -OH)(H<sub>2</sub>O)}<sub>2</sub>] $\cdot$ 7H<sub>2</sub>O (**1**) was also observed at pD 5.4 and resulted in significant acceleration of Gly-Ser hydrolysis.<sup>[8d]</sup> Catalytic reactivity towards dipeptide hydrolysis at physiological pH was also observed for the monomeric Zr<sup>IV</sup>-substituted Lindqvist POM (Me<sub>4</sub>N)<sub>2</sub>[W<sub>5</sub>O<sub>18</sub>Zr(H<sub>2</sub>O)<sub>3</sub>] (**2**).<sup>[8c]</sup> The hydrolysis of His-Ser and Gly-Ser in the presence of **2** was particularly accelerated relative to the rate of the blank reaction. The structures of **1** and **2** are presented in Figure 1.

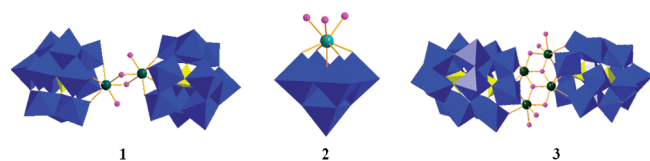


Figure 1. Schematic representation of the structures of 1–3.

Our previous studies showed that the hydrolytic reactivity of Zr<sup>IV</sup>-substituted POMs towards dipeptides is governed by the binding of the substrate to the Zr<sup>IV</sup> center on the one hand and secondary interactions between the POM skeleton and the amino acid side chain of the substrate on the other hand. These studies showed that binding of the Zr<sup>IV</sup> ion to the amide oxygen atom and the terminal amine nitrogen atom of Gly-Gly is a prerequisite for the acceleration of the hydrolysis process.<sup>[8c]</sup> However, different factors such as the size, charge, and chemical nature of the C-terminal amino acid also play a significant role. For example, the hydrolysis of dipeptides containing a Ser residue at the C-terminus is accelerated by the intramolecular attack of the Ser hydroxyl group on the amide carbonyl carbon atom to produce a five-membered cyclic transition state, which is rearranged to an ester intermediate. As a consequence, C-terminal Ser dipeptides can be autocatalytically hydrolyzed with half-lives of approximately two months.<sup>[8c]</sup> However, the intramolecular attack of the Ser hydroxyl group in dipeptides containing a Ser residue at the N-terminus results in an unfavorable four-membered cyclic transition state. Consequently, the amount of Ser-Gly hydrolyzed in the absence of catalyst is similar to that of Gly-Gly; therefore, the Ser residue at the N-terminus has little impact on the promotion of peptide bond hydrolysis in Ser-Gly. Furthermore, dipeptides containing a His residue are more readily hydrolyzed owing to electrostatic interactions between the negatively charged POM surface and

the positively charged amino acid side chain. These studies indicate that even dipeptides, which can be considered to be the smallest models for protein hydrolysis, exhibit complex behavior during peptide bond hydrolysis. Therefore, a systematic evaluation of the hydrolysis of longer peptides is required to further understand the factors that influence the selectivity and the rate of hydrolysis. Moreover, our previous studies on larger protein substrates indicate that despite the presence of an electrostatic component, the coordination of the embedded hydrolytically active metal ion to the protein chain also plays an important role.<sup>[8e,13]</sup> Therefore, smaller substrates can be of particular use in unraveling the origin of this metal-directed binding.

To further study the effect of amino acid composition on the reactivity and selectivity, the hydrolytic properties of three Zr-containing POMs towards a range of oligopeptides differing in length and the nature of the amino acids are explored in this study. For comparison, in addition to POMs **1** and **2**, we also examined the hydrolytic activity of the Wells–Dawson POM Na<sub>14</sub>[Zr<sub>4</sub>(P<sub>2</sub>W<sub>16</sub>O<sub>59</sub>)<sub>2</sub>( $\mu$ <sub>3</sub>-O)<sub>2</sub>(OH)<sub>2</sub>(H<sub>2</sub>O)<sub>4</sub>] $\cdot$ 57H<sub>2</sub>O (**3**), which is also shown in Figure 1. The POMs in this study belong to three different structural types, that is, Lindqvist, Keggin, and Wells–Dawson, and, in screening experiments, they exhibited the highest reactivity within their category towards the hydrolysis of the peptide bonds in dipeptides.

In the first step, the length of the peptide chain was increased from Gly-Gly to Gly-Gly-Gly and Gly-Gly-Gly-Gly, and preferential peptide bond hydrolysis was investigated. As the presence of Ser and His amino acids in dipeptides significantly influences the rate of peptide bond hydrolysis, the reactivity of POMs **1–3** towards Gly-Gly-His and Gly-Ser-Phe was also investigated in detail for all three POMs.

## Results and Discussion

Screening experiments with **1–3** showed that the highest reactivity towards dipeptide hydrolysis was obtained at pD 5.4 for **1** and at pD 7.4 for **2** and **3**. The stability of **1** was dependent on pD, concentration, and temperature. The partial conversion of a 2.0 mM solution of **1** into the inactive 1:2 Zr<sup>IV</sup>-Keggin species at pD 7.4 and 60 °C resulted in lower peptide bond hydrolysis rates compared with the rates observed at pD 5.4.<sup>[8d]</sup> However, complexes **2** and **3** were stable over a wide pD range (Figure S1), and the highest catalytic activities towards dipeptides were obtained at pD 7.4.<sup>[8c]</sup>

### Hydrolysis of Gly-Gly-Gly

The hydrolysis of Gly-Gly was previously investigated in the presence of **1**.<sup>[8d]</sup> At nearly neutral pH, the monomeric species [ $\alpha$ -PW<sub>11</sub>O<sub>39</sub>Zr(OH)(H<sub>2</sub>O)]<sup>4-</sup> coexists in equilibrium with **1** and is presumed to be the catalytically active species in the hydrolytic process. On the basis of the experimental NMR spectroscopy chemical shifts, the most likely hydro-

lytically active complex is formed by the coordination of Gly-Gly to the Zr<sup>IV</sup> ion through its amine nitrogen atom and amide oxygen atom. As a result, the peptide bond in Gly-Gly is activated towards nucleophilic attack by the internal Zr-bound OH nucleophile.

To better understand the catalytic activity of **1** towards peptide bond hydrolysis in oligopeptides, the hydrolysis of triglycine was investigated first. A mixture containing Gly-Gly-Gly (3G, 1.0 mM) and **1** (2.0 mM) was reacted at 60 °C and pD 5.4. The <sup>1</sup>H NMR spectra of 3G in the presence of **1** recorded at different time increments are presented in Figure S2. The assignments of the hydrolysis product glycine (G) and the intermediate products glycylglycine (2G) and cyclic glycylglycine (cGG) is based on a comparison of their chemical shifts with those of the pure products at the same pD value. The amounts of the tripeptide and all of the products observed during the course of hydrolytic reaction were determined by integration of their respective <sup>1</sup>H NMR spectroscopic resonances (Figure 2). After 1 d, the hydrolysis of 3G to equal amounts of 2G and G was observed. As was also the case for a 1:2 Zr<sup>IV</sup>-substituted Wells–Dawson POM,<sup>[8f]</sup> cyclization of 2G was observed with a maximal amount of 10% cGG. Interestingly, the total amount of 2G and cGG was smaller than that of G after 10 d, indicating that hydrolysis of 2G and 3G to G occurred. Eventually, complete hydrolysis of 3G was achieved in the presence of **1** (Scheme 1). By fitting the decrease in the concentration of 3G to a monoexponential function (Figure S3), a hydrolysis rate constant  $k_{\text{obs}} = (7.22 \pm 0.25) \times 10^{-7} \text{ s}^{-1}$  at 60 °C and pD 5.4 was obtained.

The complete hydrolysis of 3G in the presence of **2** and **3** was also observed (Figures S4 and S5). Detailed kinetic profiles for the hydrolysis of 3G in the presence of these two complexes could not be obtained due to the signal overlap in their <sup>1</sup>H NMR spectra. However, a comparison of the reactivity of these compounds towards 3G can be made on the basis of the amount of G present in solution at a certain time. After four weeks at 60 °C, ca. 65, 45, and 30% of G was formed in the presence of **1**, **3**, and **2**, respectively. A similar reactivity trend of these complexes towards 2G was observed.<sup>[8c,8d]</sup> Notably, the hydrolysis of 1.0 mM 3G in

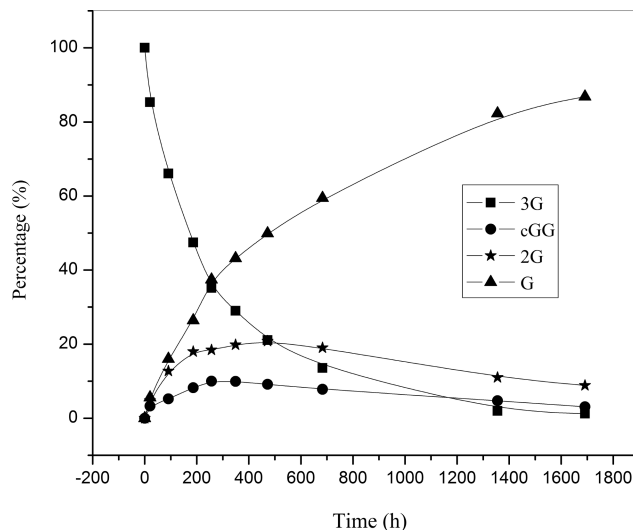
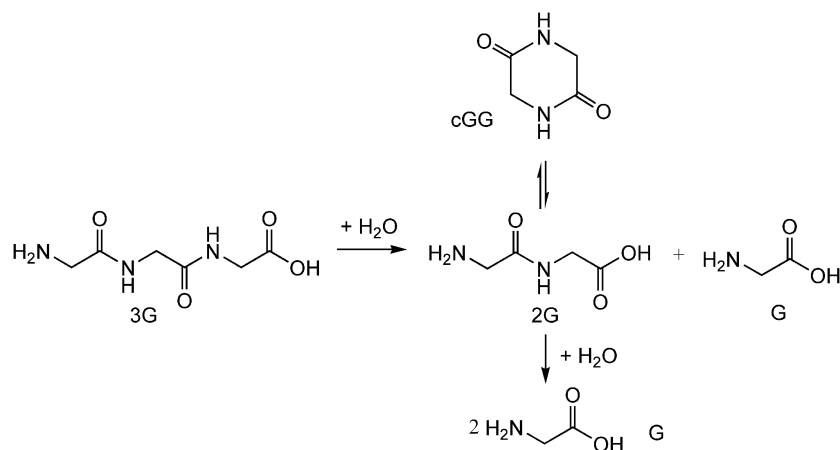


Figure 2. The percentages of 3G, 2G, cGG, and G as a function of time for the reaction between 3G (1.0 mM) and **1** (2.0 mM) at pD 5.4 and 60 °C.

the absence of **1–3** at 60 °C was very slow at both pD 5.4 and pD 7.4. After two months at 60 °C, a negligible amount of G was observed in the NMR spectrum, which suggests that the hydrolysis of 3G was due to the presence of POMs **1–3**. The presence of the tripeptides did not affect the stability of **1–3**, and the reaction mixture was completely homogeneous throughout the hydrolytic reaction. The <sup>31</sup>P NMR spectra of **1** and **3** measured in the presence of 3G after 7 d showed no extra signals compared to their <sup>31</sup>P NMR spectra in the absence of 3G; therefore, **1–3** are stable in the presence of 3G (Figures S6 and S7). The UV/Vis absorbance spectra of **2** in the absence and presence of 3G after adjustment to pD 7.4 showed an absorbance maximum at  $\lambda = 265 \text{ nm}$ , characteristic of oxygen–tungsten charge transfer in **2** (Figure S8). After 7 d at 60 °C, the UV/Vis spectrum of **2** in the presence of 3G was similar to that in the absence of the substrate (Figure S9). Similar results were also observed when **2** was used as a catalyst for the hydrolysis of the dipeptide His-Ser. In the presence of His-

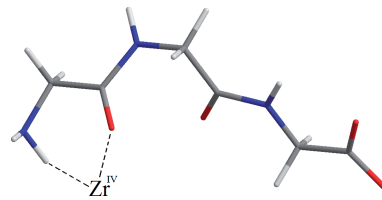


Scheme 1. Hydrolysis of 3G in the presence of **1**.

Ser, the structural integrity of **2** was further studied by small-angle X-ray scattering (SAXS). For **2**, no differences in particle size in the absence or the presence of His-Ser as well as after complete hydrolysis of His-Ser were observed. This is indicative of the stability of the complex.<sup>[8c]</sup> From these findings, we can conclude that the structure of **2** is also retained in the presence of 3G.

The acceleration of 3G hydrolysis by **1–3** indicates that the substrate interacts with the POMs. The interactions of 3G with **1–3** were investigated on the basis of the <sup>1</sup>H and <sup>13</sup>C NMR spectroscopy chemical shift changes of 3G upon the addition of **1**, **2**, or **3**. The <sup>1</sup>H NMR spectra of 3G in the absence and presence of **1** are shown in Figure S10. Slight shifts of  $\Delta\delta = 0.03$  and 0.04 ppm were observed for the resonances of 4-H and 6-H, respectively (Table S1). In addition, the <sup>13</sup>C NMR chemical shift changes of 3G in the presence of **1** are shown in Figure S11 and Table S2. The biggest shift ( $\Delta\delta = 0.28$  ppm) upon the addition of **1** was observed for the resonance of the C-5 carbon atom. The mentioned shifts in the <sup>1</sup>H and <sup>13</sup>C NMR spectra of 3G are indicative of the embedded Zr<sup>IV</sup> ion binding to the N-terminal amide oxygen atom, resulting in the polarization of the N-terminal amide bond. In addition, a shift of  $\Delta\delta = 0.05$  ppm for the resonance of the C-6 carbon atom was also observed. This could result from the binding to the terminal amine nitrogen atom. This coordination is indispensable for the hydrolysis of peptide bonds, as demonstrated in previous studies.<sup>[8f,11j,14]</sup> Notably, the differences in the <sup>13</sup>C NMR chemical shifts of the other carbon atoms were negligible. From these results, we can conclude that the acceleration of 3G hydrolysis by **1** results from the coordination of the Zr<sup>IV</sup> ion to 3G through the amine nitrogen atom and the amide carbonyl oxygen atom of the N-terminal Gly residue to form the hydrolytically active complex proposed in Scheme 2. Such binding promotes the hydrolysis of 3G to form equal amounts of 2G and G during the initial stages of hydrolysis. The hydrolysis intermediate product 2G is then hydrolyzed after forming a similar hydrolytically active complex to facilitate its hydrolysis to G, as demonstrated in our previous study.<sup>[8d]</sup> As recently experimentally detected for the first time, the monomeric form of **1** is in fast equilibrium with the dimeric structure shown in Figure 1.<sup>[15]</sup> The most stable coordination mode likely occurs through the coordination of the N-terminal amine group and the amide carbonyl group of the first residue to the monomeric form of **1**. It is worth mentioning that the presence of 3G did not cause any changes in the <sup>31</sup>P NMR spectrum of **1** (Figure S12). This could be due to the rather weak binding between the POM and the substrate or fast exchange between free and bound 3G on the <sup>31</sup>P NMR time scale.

The binding of 3G to a Zr<sup>IV</sup> center in **2** displays a similar coordination mode as that determined for **1**, but it appears to be weaker as smaller shifts were obtained for the resonances of C-5 and C-6 carbon atoms (Figure S13, Tables S3 and S4). This could explain the slower hydrolysis of 3G in the presence of **2** compared to that in the presence of **1**. However, in the presence of **3**, the coordination of 3G



Scheme 2. Hydrolytically active complex between 3G and a Zr<sup>IV</sup> center for the hydrolysis of 3G in the presence of **1**.

appears to be more complicated (Figure S14 and Table S5). The resonances of all of the carbon atoms of 3G were shifted in the presence of **3**. In addition, the resonances of all three CH<sub>2</sub> protons of 3G were shifted, and the biggest shift ( $\Delta\delta = 0.09$  ppm) was for the 4-H protons (Figure S15 and Table S6). These shifts indicate the presence of multiple coordination modes between 3G and POM **3**, possibly because four Zr<sup>IV</sup> ions are available for interaction.

### Hydrolysis of Gly-Gly-Gly-Gly

The hydrolysis of the tetrapeptide Gly-Gly-Gly-Gly (4G) is interesting because this peptide possesses one internal peptide bond, unlike Gly-Gly and Gly-Gly-Gly. The hydrolysis of 4G (1.0 mM) catalyzed by **1** (2.0 mM) was studied at 60 °C and pD 5.4. The <sup>1</sup>H NMR spectra of the reaction at different time increments are presented in Figure S16. The assignments of the intermediate products and hydrolysis product glycine are based on a comparison of their chemical shifts with those of the pure products (Gly, Gly-Gly, and Gly-Gly-Gly) at the same pD value. The amounts of 4G and all of the products observed during the course of hydrolytic reaction were determined by integration of their respective <sup>1</sup>H NMR spectroscopic resonances (Figure 3). Initially, only the hydrolysis of 4G to 3G and G was observed during the first 24 h at 60 °C. The presence of 2G, which could result from the hydrolysis of the N-

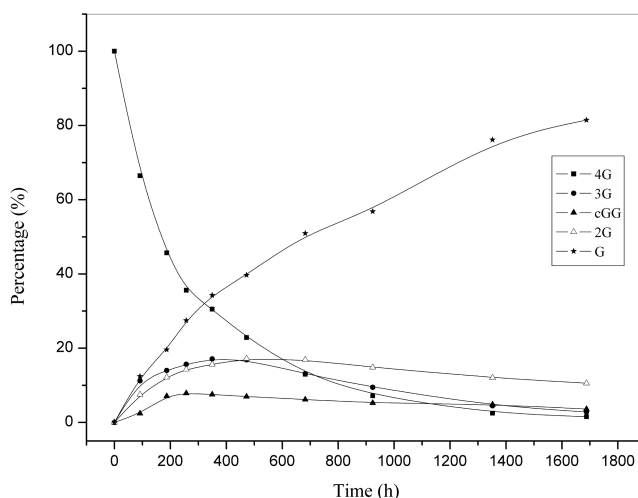


Figure 3. Percentages of 4G, 3G, 2G, cGG, and G as a function of time for the reaction between 4G (1.0 mM) and **1** (2.0 mM) at pD 5.4 and 60 °C.

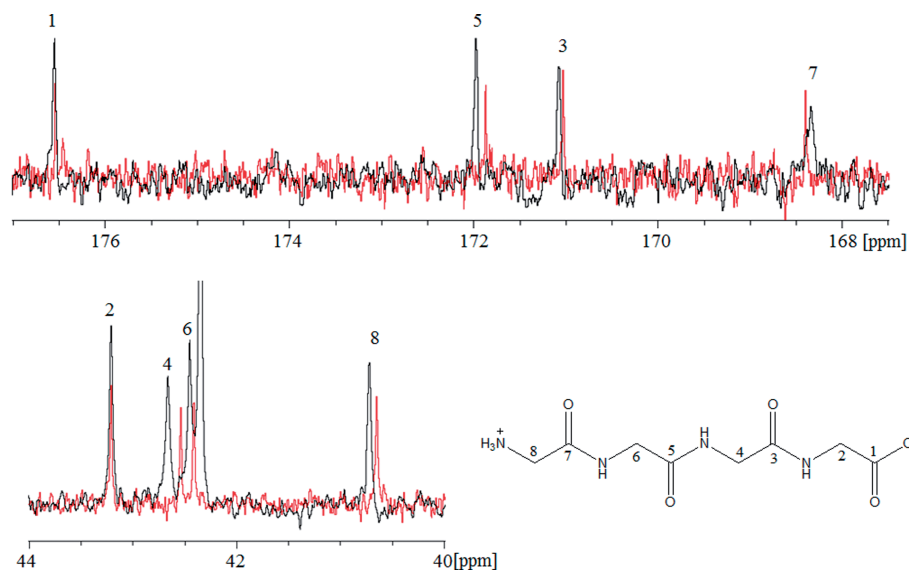
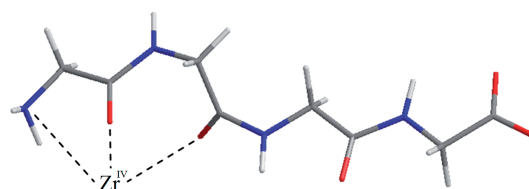
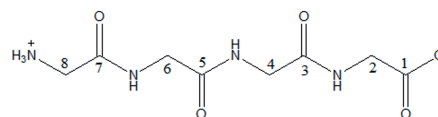


Figure 4.  $^{13}\text{C}$  NMR spectra of 4G in the absence (black) and presence (red) of **1** at pD 7.4 (the signal at  $\delta = 42.4$  ppm belongs to the  $\text{CH}_2$  carbon atom of the ethyl group in the counterion).

terminal peptide bond of 3G or the internal peptide bond of 4G, was only observed after 24 h, and its maximal amount of 17% was obtained after 20 d. These findings indicate that the hydrolysis of the N-terminal peptide bond of 4G is more favorable than the hydrolysis of the internal or C-terminal peptide bonds of 4G. The tetrapeptide 4G was eventually fully hydrolyzed to G. The observed rate constant for 4G hydrolysis of  $(6.75 \pm 0.30) \times 10^{-7} \text{ s}^{-1}$  at pD 5.4 and 60 °C was calculated from the decrease in concentration of 4G (Figure S17).

The binding between 4G and **1** was further studied by NMR spectroscopy. The  $^1\text{H}$  NMR spectroscopic data of 4G in the presence and absence of **1** are shown in Figure S18 and Table S7. The biggest shifts of  $\Delta\delta = 0.07$  and 0.06 ppm were obtained for the 6-H and 8-H protons, respectively. In addition, upon the addition of **1**, bigger chemical shift changes were observed for the C-5 and C-7 amide carbonyl carbon atoms than for the C-3 amide carbonyl carbon atom (Figure 4 and Table S8). In addition, a shift of  $\Delta\delta = 0.07$  ppm was also observed for the N-terminal methylene carbon atom, and no changes were found for the carboxylate carbon atom. The unaffected chemical shift of the carboxylate carbon atom upon the addition of **1** indicates that the carboxylate oxygen atom is not involved in coordination to the POM. These changes in the  $^1\text{H}$  and  $^{13}\text{C}$  chemical shifts upon the addition of **1** are likely a consequence of complex formation between the  $\text{Zr}^{\text{IV}}$  center and 4G through the terminal amine nitrogen atom and the first and second amide carbonyl oxygen atoms from the N-terminus, as shown in Scheme 3. This type of binding facilitates the cleavage of the N-terminal and internal peptide bonds of 4G to form the intermediate hydrolysis products 3G and 2G, as discussed above.

In the presence of **2** and **3**, complete hydrolysis of 4G was achieved at pD 7.4 and 60 °C (Figures S19 and S20). After 28 d, ca. 55, 45, and 30% of G was formed in the



Scheme 3. Hydrolytically active complex between 4G and a  $\text{Zr}^{\text{IV}}$  center for the hydrolysis of 4G in the presence of **1**.

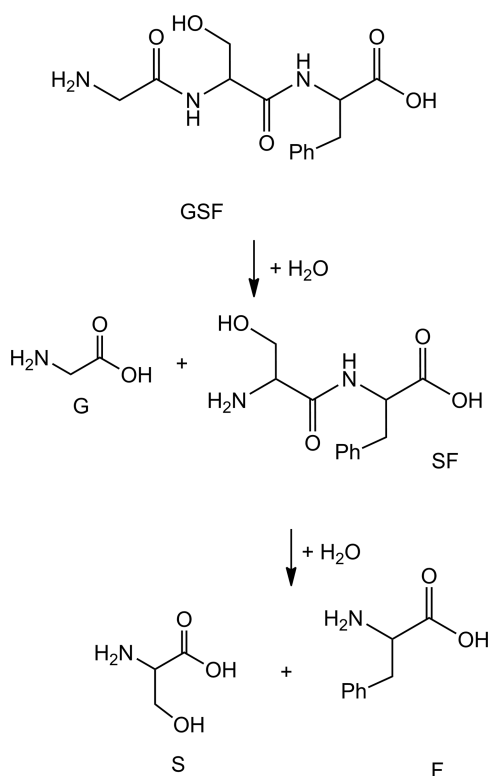
presence of **1**, **3**, and **2**, respectively. Thus, the reactivity of  $\text{Zr}^{\text{IV}}$ -substituted POMs towards 4G can be arranged in the order  $\mathbf{1} > \mathbf{3} > \mathbf{2}$ . The hydrolysis of 4G in the absence of **1–3** at 60 °C and pD 5.4 or 7.4 was also studied. After 28 d, no free G could be observed in solution, and only ca. 3% of the tetrapeptide was hydrolyzed after two months; this suggests that the presence of  $\text{Zr}^{\text{IV}}$ -substituted POMs accelerates the hydrolysis of 4G.

The binding of 4G to **2** and **3** was also studied on the basis of changes in the  $^{13}\text{C}$  NMR spectrum of 4G upon the addition of these POMs. In the presence of **2**, the binding is very weak, as only small shifts were obtained (Figure S21 and Table S9). This could explain why **2** exhibits the lowest reactivity of the examined  $\text{Zr}^{\text{IV}}$ -substituted POMs towards 4G hydrolysis. The  $^{13}\text{C}$  NMR spectroscopic data of 4G in the presence of **3** show big shifts of the resonances of all carbon atoms (Figure S22 and Table S10). The  $^{13}\text{C}$  NMR chemical shift changes for all of the carbon atoms of 4G were also observed in the presence of the 1:2  $\text{Zr}^{\text{IV}}$  Wells–Dawson POM.<sup>[8f]</sup> This suggests that there is no preferred coordination mode and, consequently, the hydrolysis is less efficient and the reaction rate is lower than those for **1**.

### Hydrolysis of Gly-Ser-Phe

The hydrolysis of Gly-Ser-Phe (GSF, 1.0 mM) in the presence of **1** (2.0 mM) was studied at 60 °C and pD 5.4.

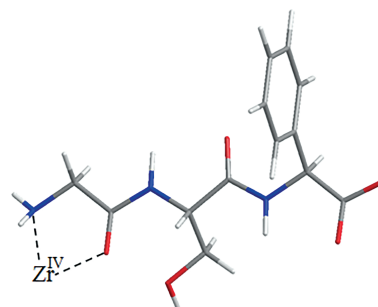
The  $^1\text{H}$  NMR spectra of GSF in the presence of **1** at various reaction times are shown in Figure S23. The intermediate product Ser-Phe (SF) and the hydrolysis products glycine (G), serine (S), and phenylalanine (F) were assigned on the basis of a comparison of their chemical shifts with those of pure products at the same pD value. On the basis of the integration of the respective  $^1\text{H}$  NMR spectroscopic resonances, the amounts of the GSF and all of the products observed during the course of hydrolytic reaction were determined (Figure S24). The observation of only G and SF during the first stages of the reaction indicates that GSF is initially hydrolyzed at the Gly-Ser bond. Interestingly, Gly-Ser was not observed throughout the reaction. These findings indicate that the hydrolysis of GSF at the Ser-Phe bond to produce GS and F did not occur. Interestingly, the observation of S and F in the NMR spectra indicates that Ser-Phe was partially hydrolyzed into S and F in the next step. The hydrolysis reaction of GSF is presented in Scheme 4. As can be seen from Figure S23, the complete hydrolysis of GSF to G and SF was achieved, but SF was still prominent in the mixture. By fitting the decrease in the concentration of GSF to a monoexponential function, a rate constant  $k_{\text{obs}}$  of  $(10.14 \pm 0.04) \times 10^{-7} \text{ s}^{-1}$  was obtained (Figure S25). The observed selectivity for the Gly-Ser bond can be explained by the nucleophilic nature of the hydroxyl group of the Ser residue. The internal attack on the carbonyl carbon atom of the Gly residue through an N $\rightarrow$ O acyl rearrangement results in an ester intermediate, which can be more readily hydrolyzed. Consequently, GSF can be autocatalytically hydrolyzed. After two months, 5% of G

Scheme 4. Hydrolysis of GSF in the presence of **1**.

formed at pD 5.4 and 1% formed at pD 7.4 in the absence of **1** (Figure S26). The hydrolysis of Gly-Ser by **1** at pD 5.4 and 60 °C is approximately six times faster than the hydrolysis of Gly-Ser-Phe.<sup>[8d]</sup> The slower hydrolysis of Gly-Ser-Phe compared to that of Gly-Ser is most likely caused by the presence of the bulky phenyl group in the side chain of the Gly-Ser-Phe tripeptide. The bulkiness of the Phe residue sterically impedes the intramolecular attack of the Ser hydroxyl group on the amide carbonyl carbon atom.

The hydrolysis of GSF in the presence of **2** and **3** was also observed (Figures S27 and S28); however, detailed kinetic studies for the reactions in the presence of these two complexes cannot be obtained owing to signal overlap in the  $^1\text{H}$  NMR spectra. After 10 d of reaction, ca. 55, 31, and 20% of G was found in the presence of **1**, **3**, and **2**, respectively; therefore, the same reactivity tendency as that demonstrated for 3G and 4G was observed for GSF.

The coordination of GSF to **1** was examined on the basis of the shifts in the  $^1\text{H}$  and  $^{13}\text{C}$  NMR spectra of GSF upon the addition of **1**. The  $^{13}\text{C}$  NMR spectra of GSF in the absence and presence of **1** are shown in Figure S29. The changes in the  $^{13}\text{C}$  NMR chemical shifts of GSF induced by the addition of **1** are summarized in Table S11. It can be clearly seen that the presence of **1** caused a shift of  $\Delta\delta = 0.28$  ppm for the resonance of the C-5 carbon atom, indicative of the binding of the  $\text{Zr}^{\text{IV}}$  center to the amide oxygen atom of the Gly residue. Moreover, the shift of  $\Delta\delta = 0.07$  ppm for the C-6 carbon atom upon the addition of **1** is a result of the binding of the  $\text{Zr}^{\text{IV}}$  center to the amine nitrogen atom. The binding of the amine nitrogen atom to a metal ion is indispensable for the acceleration of peptide bond hydrolysis, as extremely slow hydrolysis rates were obtained for N-terminal-protected dipeptides.<sup>[8f,11j,14]</sup> The resonances of all of the other carbon atoms were almost unaffected by the presence of **1**. Additionally, the  $^1\text{H}$  NMR spectra of GSF show a significant shift of  $\Delta\delta = 0.06$  ppm for the resonance of the  $\text{H}_\alpha$  proton of the Gly residue, which supports the binding between GSF and **1** through the amine nitrogen atom and the amide carbonyl oxygen atom of the Gly residue (Figure S30). From these results, we can conclude that the enhancement in hydrolysis of GSF is due to the complexation of the  $\text{Zr}^{\text{IV}}$  center to GSF to form the hydrolytically active complex proposed in Scheme 5. The binding results are in accordance with the kinetic data for

Scheme 5. The proposed hydrolytically active GSF- $\text{Zr}^{\text{IV}}$  complex for the hydrolysis of GSF in the presence of **1**.

GSF hydrolysis, in which only the GS bond was initially hydrolyzed, and the SF bond was hydrolyzed only after the complete hydrolysis of GSF to G and SF.

### Hydrolysis of Gly-Gly-His

A mixture containing Gly-Gly-His (GGH, 1.0 mM) and **1** (2.0 mM) was reacted at 60 °C and pD 5.4. The <sup>1</sup>H NMR spectra of GGH in the presence of **1** recorded at different time increments are presented in Figure S31. The assignments of the hydrolysis products glycine (G) and histidine (H) as well as the intermediate products glycyglycine (2G) and glycyhistidine (GH) are based on comparisons of their chemical shifts with those of pure products at the same pD value. The amounts of the tripeptide and all of the products observed during the course of the hydrolytic reaction were determined by integration of their respective <sup>1</sup>H NMR spectroscopic resonances (Figure 5). After 20 h of reaction, approximately 6% of G, 5% of GH, and 0.5% of H were found, whereas no 2G was observed in the NMR spectrum. This result indicates that the hydrolysis of GGH initially occurred at the GG peptide bond to form G and GH and that GH further hydrolyzed to G and H [Scheme 6, Pathway (1)]. The hydrolysis of GGH to 2G and H [Scheme 6, Pathway (2)] in the presence of **1** was also observed at latter stages of the reaction. After 95 h, ca. 10% of GGH hydrolyzed to G + GH and 3% hydrolyzed to 2G + H; therefore, both pathways run in parallel during the hydrolysis of GGH. In addition, as the amount of GH was always greater than that of 2G throughout the reaction, the N-terminus peptide bond is more susceptible to hydrolysis than the C-terminus peptide bond in GGH. Complete hydrolysis of GGH was obtained with an observed rate con-

stant of  $(6.25 \pm 0.21) \times 10^{-7} \text{ s}^{-1}$ . Interestingly, in the control reactions at 60 °C and pD 5.4 or pD 7.4, only Pathway (1) was observed for the hydrolysis of GGH. After two months, only ca. 0.5% of GGH hydrolyzed to G and GH at pD 5.4, whereas ca. 2% hydrolyzed at pD 7.4; therefore, the hydrolysis of GGH was significantly facilitated by **1**.

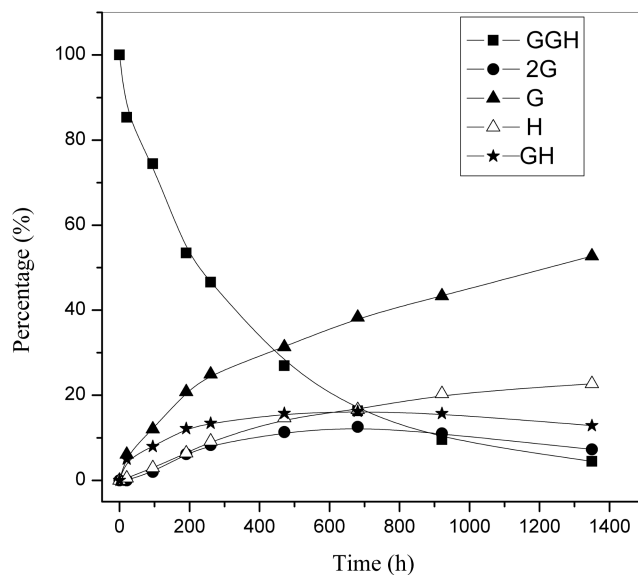
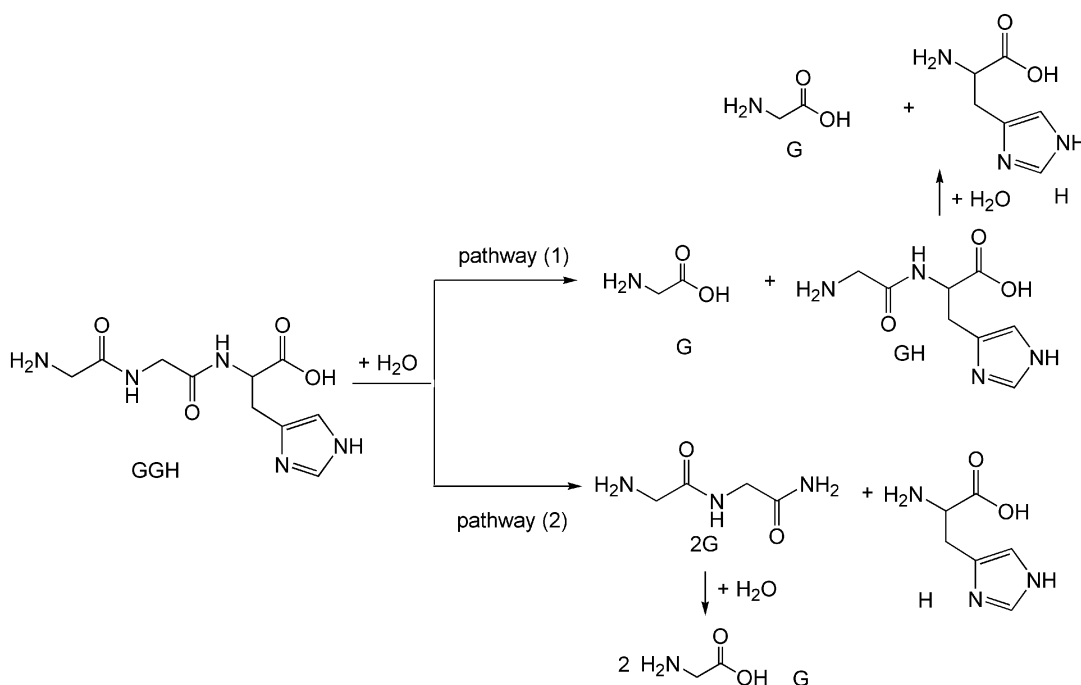


Figure 5. Percentages of GGH, 2G, GH, H, and G as a function of time for the reaction between GGH (1.0 mM) and **1** (2.0 mM) at pD 5.4 and 60 °C.

The interactions between GGH and **1** were studied by <sup>13</sup>C NMR spectroscopy by recording the spectra of GGH in the absence and presence of **1** (Figure S32). The changes in the <sup>13</sup>C NMR chemical shifts of GGH induced upon the



Scheme 6. Hydrolysis of GGH in the presence of **1**.

addition of **1** are summarized in Table 1. A shift of  $\Delta\delta = 0.28$  ppm for the resonance of the C-5 carbon atom was observed, and the resonance of the C-3 carbon atom was shifted by  $\Delta\delta = 0.11$  ppm. This could be a result of the binding of the Zr<sup>IV</sup> center to the two amide oxygen atoms, which would polarize the amide carbon atoms and make them more susceptible towards nucleophilic attack by water. The observance of a stronger binding of the Zr<sup>IV</sup> center to the amide oxygen atom of the terminal Gly residue and the amine nitrogen atom explains the dominance of Pathway (1) for the hydrolysis of GGH. In addition to the expected shifts, the resonances of all of the carbon atoms of the side chain were also significantly shifted. This is most likely a consequence of the electrostatic interaction between the positively charged side chain and the negatively charged POM surface as well as the binding of the Zr<sup>IV</sup> center to the imidazole nitrogen atom, as observed for the dipeptide Gly-His.<sup>[8b]</sup> As demonstrated previously by Harford and co-workers, the binding of GGH to Cu<sup>II</sup> and Ni<sup>II</sup> centers lowered the pK<sub>a</sub> values of the amide nitrogen atoms, resulting in the deprotonation of the amide nitrogen atoms and forming complexes through the amine nitrogen atom, the two amide nitrogen atoms, and the imidazole N-3 nitrogen atom.<sup>[16]</sup> In the presence of **1**, the resonances of the C-2 and C-4 carbon atoms were also shifted by  $\Delta\delta = 0.33$  ppm, due to the complexation of the amide nitrogen atoms or the carbonyl oxygen atoms. Additionally, the resonance of the carboxylate group was also affected upon the addition of **1**, which indicates that this carboxylate group is involved in coordination with the Zr<sup>IV</sup> center. The coordination of the carboxylate group of Gly-His to the Zr<sup>IV</sup> center in Zr<sup>IV</sup>-substituted Wells–Dawson-type POMs was previously observed.<sup>[8b]</sup> These findings suggest that multiple coordination modes between GGH and **1** result in the formation of different complexes with structures that are difficult to elucidate solely from <sup>13</sup>C NMR spectroscopic data. However, for the reaction Pathways (1) and (2) shown in Scheme 6 to occur, the interaction between the Zr<sup>IV</sup> center and the C-3 and C-5 carbonyl oxygen atoms must occur, as is consistent with the observed shifts in Figure S32. The shifts of the carbon resonances in the imidazole region suggest additional coordination to N-3 in the side chain of His, which facilitates the anchoring of the Zr<sup>IV</sup> center to the polypeptide.

The hydrolysis of GGH in the presence of **2** and **3** was further investigated, and the <sup>1</sup>H NMR spectra of GGH in the presence of **2** and **3** recorded at different time increments are presented in Figures S33 and S34, respectively. As can be seen from these two figures, complete hydrolysis of GGH occurred. However, detailed kinetic profiles for the hydrolysis of GGH in the presence of these two complexes could not be obtained due to signal overlap in their <sup>1</sup>H NMR spectra. The interactions between GGH and the Zr<sup>IV</sup> ions in **2** and **3** were also explored by <sup>13</sup>C NMR spectroscopy. The <sup>13</sup>C NMR spectra of GGH before and after addition of **3** are shown in Figure S35. The <sup>13</sup>C NMR chemical shifts of GGH are summarized in Table S12. Similarly to the presence of **1**, the presence of **3** results in a

Table 1. <sup>13</sup>C NMR chemical shifts [ppm] of GGH (15.0 mM) in the absence and presence of **1** (2.0 mM) at pD 7.4.

<sup>13</sup> C NMR	GGH	GGH + <b>1</b>	$\Delta\delta$
$\delta_1$	176.76	176.47	0.29
$\delta_2$	54.54	54.21	0.33
$\delta_3$	168.35	168.24	0.11
$\delta_4$	42.33	42.66	0.33
$\delta_5$	170.28	170.56	0.28
$\delta_6$	40.70	30.23	0.47
$\delta_7$	28.07	27.54	0.53
$\delta_8$	130.97	130.02	0.95
$\delta_9$	117.34	117.18	0.16
$\delta_{10}$	134.33	134.90	0.57

greater shift of the resonance of the C-5 carbon atom than that of the C-3 carbon atom, indicating stronger interaction with the amide oxygen atom of the terminal Gly residue than that with the central Gly residue. The coordination to the amine nitrogen atom was also observed, and this would assist the hydrolysis by Pathway (1). Analogous binding at the amide oxygen atoms and the amine nitrogen atom was also achieved in the presence of **2**, but, as with all other oligopeptides in this study, the interaction was weaker as smaller shifts were obtained (Figure S36 and Table S13). In addition to these expected shifts for the acceleration of the hydrolysis of the peptide bonds in GGH, similar shifts of the resonances of all other carbon atoms to those observed in the presence of **1** were also obtained in the presence of **2** and **3**. These results demonstrate multiple coordination modes for the complexation of Zr<sup>IV</sup>-substituted POMs to GGH, similarly to the multiple coordination modes that were observed between oxovanadium and this tripeptide.<sup>[17]</sup>

## Conclusions

In this paper, we report the hydrolysis of the oligopeptides triglycine, tetraglycine, glycylglycylhistidine, and glycylserylphenylalanine by a series of Zr<sup>IV</sup>-substituted POMs **1–3** under mildly acidic and neutral conditions. Homogeneous peptide bond hydrolysis was achieved for all of the oligopeptides in the presence of all three POMs.

Of the three POMs under investigation, the Zr<sup>IV</sup>-substituted Keggin POM **1** was the most-active POM. Hydrolysis rates in the order **1** > **3** > **2** were observed for all oligopeptides, and the hydrolysis with **1** was typically twice as fast as that with **2**. This higher reactivity might be explained by the specific peptide coordination observed in the presence of **1**. Typically, the N-terminal amine group and the amide carbonyl group of the first Gly residue coordinate to the Zr<sup>IV</sup> center of **1** and, consequently, the first peptide bond is activated and hydrolyzed. This type of coordination was also observed in the presence of **2** and **3**; however, as the observed changes in the <sup>13</sup>C NMR shifts were smaller, the interactions are either weaker or less of the active complex forms in solution, and the hydrolysis rates are lower. The reason for the multiple coordination modes observed between all of the oligopeptides and POM **3** could be that the dimeric form of POM **3** contains four

Zr<sup>IV</sup> ions, which offer multiple coordination possibilities. Furthermore, it is plausible that, similarly to **1**, this POM exists in a monomer/dimer equilibrium that is too fast to observe on the NMR time scale.<sup>[18]</sup> This equilibrium would result in a monomeric complex bearing two Zr<sup>IV</sup> centers with several aqua ligands that could be readily substituted by oligopeptide substrates. We are currently performing theoretical calculations on the possible equilibria of **3** to shed more light on this issue.

For the oligopeptides, the extension of the chain length from 2G to 3G and 4G still resulted in complete hydrolysis; therefore, POMs **1–3** can fully hydrolyze longer peptide chains. On the basis of the preferential binding of **1** at the N-terminal Gly residues in 3G and the fact that no 2G is observed during the initial stages of 4G hydrolysis, in the absence of any specific secondary interactions, **1** likely starts to hydrolyze Gly oligopeptides at their N-terminus, and the hydrolysis then progresses further downstream until complete hydrolysis is achieved. The rate of oligopeptide hydrolysis in the presence of **1** was fastest for the tripeptide GSF, in which the Gly-Ser bond was preferentially hydrolyzed. This further demonstrates the beneficial role that Ser residues play as internal nucleophiles in peptide hydrolysis. However, the presence of bulky neighboring residues such as Phe impedes the active role that Ser plays in GSF hydrolysis.

The demonstrated trend in selectivity can be best compared to that observed for oxidized insulin chain B.<sup>[12]</sup> The selectivity of hydrolysis was also driven by coordination chemistry between the Zr<sup>IV</sup> ion in the POM and the polypeptide, whereas no evidence of specific electrostatic interactions, as is the case for protein hydrolysis, was observed. This can be explained by the lack of any tertiary structure in the substrates under study. The results obtained in this study are of importance for the design of artificial peptidase agents for biotechnology applications in which frequently denatured or polypeptide chains need to be selectively hydrolyzed.

## Experimental Section

**Chemicals:** Complexes **1**, **2**, and **3** were synthesized according to the procedures reported previously.<sup>[8d,19]</sup> Gly-Gly-Gly (3G), Gly-Gly-Gly-Gly (4G), Gly-Ser-Phe (GSF), Gly-Gly-His (GGH), D<sub>2</sub>O, DCl, and NaOD were purchased from Sigma–Aldrich.

**Measurements:** The <sup>1</sup>H NMR spectra were recorded with a Bruker Advance 400 spectrometer, and [D<sub>4</sub>]sodium 3-(trimethylsilyl)propionate ([D<sub>4</sub>]TMSP) was used as an internal reference. The <sup>13</sup>C NMR spectra were recorded with a Bruker Advance 400 spectrometer. As a reference, tetramethylsilane (TMS) in an internal reference tube was used. The <sup>31</sup>P NMR spectra were recorded with a Bruker Advance 400 spectrometer, and 25% H<sub>3</sub>PO<sub>4</sub> in H<sub>2</sub>O in an internal reference tube was used as a reference.

**Hydrolysis Studies:** The hydrolysis reaction mixtures typically contained oligopeptide (1.0 mM), **1–3** (2.0 mM), and [2,2,3,3-D<sub>4</sub>]TMSP in D<sub>2</sub>O. The pD of the reaction mixtures was adjusted to 5.4 or 7.4 with minor amounts of DCl (1.0 M) or NaOD (1.0 M). The pH meter reading was corrected by the equation: pD = pH + 0.41.<sup>[20]</sup>

The reaction mixtures were kept at 60 °C, and the <sup>1</sup>H NMR spectra were recorded after mixing and after different time increments. The hydrolysis products were identified by comparison of the <sup>1</sup>H NMR chemical shifts with those of pure compounds at the same pD value.

**Supporting Information** (see footnote on the first page of this article): <sup>1</sup>H, <sup>13</sup>C, and <sup>31</sup>P NMR spectra; kinetic profiles for hydrolysis reactions; UV/Vis absorbance spectra of **2** in the absence and presence of 3G.

## Acknowledgments

H. G. T. L. thanks the Vietnamese Government for support. KU Leuven is thanked for doctoral fellowships to H. G. T. L. and T. N. P. V. (START1/09/028). G. A. thanks the Fonds voor Wetenschappelijk Onderzoek – Vlaanderen (FWO) for the postdoctoral fellowship.

- [1] a) A. Proust, R. Thouvenot, P. Gouzerh, *Chem. Commun.* **2008**, 1837–1852; b) D. L. Long, R. Tsunashima, L. Cronin, *Angew. Chem. Int. Ed.* **2010**, *49*, 1736–1758; *Angew. Chem.* **2010**, *122*, 1780.
- [2] a) K. Nomiya, Y. Sakai, S. Matsunaga, *Eur. J. Inorg. Chem.* **2011**, 179–196; b) B. Keita, L. Nadjo, *J. Mol. Catal. A* **2007**, *262*, 190–215.
- [3] a) M. T. Pope, A. Muller, *Angew. Chem. Int. Ed. Engl.* **1991**, *30*, 34–48; *Angew. Chem.* **1991**, *103*, 56; b) H. Stephan, M. Kubeil, F. Emmerling, C. E. Müller, *Eur. J. Inorg. Chem.* **2013**, 1585–1594; c) M. Ammam, *J. Mater. Chem. A* **2013**, *1*, 6291–6312; d) Y. F. Song, R. Tsunashima, *Chem. Soc. Rev.* **2012**, *41*, 7384–7402; e) A. Ogata, S. Mitsui, H. Yanagie, H. Kasano, T. Hisa, T. Yamase, M. Eriguchi, *Biomed. Pharmacother.* **2005**, *59*, 240–244; f) T. Yamase, *J. Mater. Chem.* **2005**, *15*, 4773–4782; g) H. Stephan, M. Kubeil, F. Emmerling, C. E. Müller, *Eur. J. Inorg. Chem.* **2013**, 1585–1594; h) S. Mitsui, A. Ogata, H. Yanagie, H. Kasano, T. Hisa, T. Yamase, M. Eriguchi, *Biomed. Pharmacother.* **2006**, *60*, 353–358.
- [4] J. T. Rhule, C. L. Hill, D. A. Judd, R. F. Schinazi, *Chem. Rev.* **1998**, *98*, 327–358.
- [5] a) N. Mizuno, K. Kamata, K. Yamaguchi, *Top. Catal.* **2010**, *53*, 876–893; b) N. Mizuno, K. Yamaguchi, K. Kamata, *Coord. Chem. Rev.* **2005**, *249*, 1944–1956; c) O. A. Kholdeeva, *Eur. J. Inorg. Chem.* **2013**, 1595–1605.
- [6] a) Z. Huang, Z. Luo, Y. V. Geletii, J. W. Vickers, Q. Yin, D. Wu, Y. Hou, Y. Ding, J. Song, D. G. Musaev, C. L. Hill, T. Lian, *J. Am. Chem. Soc.* **2011**, *133*, 2068–2071; b) Y. V. Geletii, B. Botar, P. Kögerler, D. A. Hillesheim, D. G. Musaev, C. L. Hill, *Angew. Chem. Int. Ed.* **2008**, *47*, 3896–3899; *Angew. Chem.* **2008**, *120*, 3960; c) M. Orlandi, R. Argazzi, A. Sartorel, M. Carraro, G. Scorrano, M. Bonchio, F. Scandola, *Chem. Commun.* **2010**, *46*, 3152–3154; d) D. Lieb, A. Zahl, E. F. Wilson, C. Streb, L. C. Nye, K. Meyer, I. Ivanovic-Burmazovic, *Inorg. Chem.* **2011**, *50*, 9053–9058.
- [7] a) C. Boglio, G. Lemièrre, B. Hasenknopf, S. Thorimbert, E. Lacôte, M. Malacria, *Angew. Chem. Int. Ed.* **2006**, *45*, 3324–3327; *Angew. Chem.* **2006**, *118*, 3402–3405; b) H. El Moll, B. Nohra, P. Mialane, J. Marrot, N. Dupré, B. Riflade, M. Malacria, S. Thorimbert, B. Hasenknopf, E. Lacôte, P. A. Aparicio, X. López, J. M. Poblet, A. Dolbecq, *Chem. Eur. J.* **2011**, *17*, 14129–14138; c) C. Boglio, K. Micoine, P. Remy, B. Hasenknopf, S. Thorimbert, E. Lacôte, M. Malacria, C. Afonso, J. C. Tabet, *Chem. Eur. J.* **2007**, *13*, 5426–5432; d) N. Dupré, P. Rémy, K. Micoine, C. Boglio, S. Thorimbert, E. Lacôte, B. Hasenknopf, M. Malacria, *Chem. Eur. J.* **2010**, *16*, 7256–7264.
- [8] a) S. Vanhaecht, G. Absillis, T. N. Parac-Vogt, *Dalton Trans.* **2012**, *41*, 10028–10034; b) S. Vanhaecht, G. Absillis, T. N. Parac-Vogt, *Dalton Trans.* **2013**, *42*, 15437–15446; c) H. G. T. Ly,

- G. Absillis, S. R. Bajpe, J. A. Martens, T. N. Parac-Vogt, *Eur. J. Inorg. Chem.* **2013**, 4601–4611; d) H. G. T. Ly, G. Absillis, T. N. Parac-Vogt, *Dalton Trans.* **2013**, 42, 10929–10938; e) K. Stroobants, G. Absillis, E. Moelants, P. Proost, T. N. Parac-Vogt, *Chem. Eur. J.* **2014**, 20, 3894–3897; f) G. Absillis, T. N. Parac-Vogt, *Inorg. Chem.* **2012**, 51, 9902–9910; g) K. Stroobants, G. Absillis, P. S. Shestakova, R. Willem, T. N. Parac-Vogt, *J. Cluster Sci.* **2014**, 25, 855–866.
- [9] a) A. Radzicka, R. Wolfenden, *J. Am. Chem. Soc.* **1996**, 118, 6105–6109; b) R. A. R. Bryant, D. E. Hansen, *J. Am. Chem. Soc.* **1996**, 118, 5498–5499; c) R. M. Smith, D. E. Hansen, *J. Am. Chem. Soc.* **1998**, 120, 8910–8913.
- [10] H. Sigel, R. B. Martin, *Chem. Rev.* **1982**, 82, 385–426.
- [11] a) J. W. Jeon, S. J. Son, C. E. Yoo, I. S. Hong, J. Suh, *Bioorg. Med. Chem.* **2003**, 11, 2901–2910; b) N. M. Milović, N. M. Kostic, *J. Am. Chem. Soc.* **2003**, 125, 781–788; c) T. N. Parac, N. M. Kostic, *Inorg. Chem.* **1998**, 37, 2141–2144; d) T. N. Parac, N. M. Kostic, *J. Am. Chem. Soc.* **1996**, 118, 5946–5951; e) T. N. Parac, N. M. Kostic, *J. Am. Chem. Soc.* **1996**, 118, 51–58; f) T. N. Parac, G. M. Ullmann, N. M. Kostic, *J. Am. Chem. Soc.* **1999**, 121, 3127–3135; g) M. Yashiro, Y. Sonobe, A. Yamamura, T. Takarada, M. Komiyama, Y. Fujii, *Org. Biomol. Chem.* **2003**, 1, 629–632; h) M.-J. Rhee, C. B. Storm, *J. Inorg. Biochem.* **1979**, 11, 17–24; i) M. T. Bordignon Luiz, B. Szpoganicz, M. Rizzoto, M. G. Basallote, A. E. Martell, *Inorg. Chim. Acta* **1999**, 287, 134–141; j) T. Takarada, M. Yashiro, M. Komiyama, *Chem. Eur. J.* **2000**, 6, 3906–3913; k) M. Kasai, K. B. Grant, *Inorg. Chem. Commun.* **2008**, 11, 521–525; l) M. Kassai, R. G. Ravi, S. J. Shealy, K. B. Grant, *Inorg. Chem.* **2004**, 43, 6130–6132.
- [12] A. Sap, G. Absillis, T. N. Parac-Vogt, *Dalton Trans.* **2015**, 44, 1539–1548.
- [13] K. Stroobants, V. Goovaerts, G. Absillis, G. Bruylants, E. Moelants, P. Proost, T. N. Parac-Vogt, *Chem. Eur. J.* **2014**, 20, 9567–9577.
- [14] P. H. Ho, K. Stroobants, T. N. Parac-Vogt, *Inorg. Chem.* **2011**, 50, 12025–12033.
- [15] L. Thi Kim Nga, G. Absillis, P. Shestakova, T. N. Parac-Vogt, *Eur. J. Inorg. Chem.* **2014**, 5276–5284.
- [16] C. Harford, B. Sarkar, *Acc. Chem. Res.* **1997**, 30, 123–130.
- [17] E. Garribba, G. Micera, E. Lodyga-Chruscinska, D. Sanna, G. Sanna, *Eur. J. Inorg. Chem.* **2005**, 4953–4963.
- [18] T. K. N. Luong, P. Shestakova, T. T. Mihaylov, G. Absillis, K. Pierloot, T. N. Parac-Vogt, *Chem. Eur. J.* **2015**, 21, 4428–4439.
- [19] a) H. Carabineiro, R. Villanneau, X. Carrier, P. Herson, F. Lemos, F. R. Ribeiro, A. Proust, M. Che, *Inorg. Chem.* **2006**, 45, 1915–1923; b) A. J. Gaunt, I. May, D. Collison, K. Travis Holman, M. T. Pope, *J. Mol. Struct.* **2003**, 656, 101–106; c) Y. Saku, Y. Sakai, K. Nomiya, *Inorg. Chem. Commun.* **2009**, 12, 650–652.
- [20] P. K. Glasoe, F. A. Long, *J. Phys. Chem.* **1960**, 64, 188.

Received: February 13, 2015

Published Online: ■

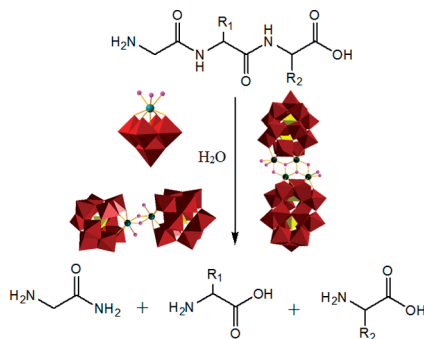
## Polymetalates

H. G. T. Ly, G. Absillis,  
T. N. Parac-Vogt\* ..... 1–11



Comparative Study of the Reactivity of Zirconium(IV)-Substituted Polyoxometalates towards the Hydrolysis of Oligopeptides

**Keywords:** Enzyme mimics / Peptidases / Oligopeptides / Polyoxometalates / Hydrolysis / Zirconium



The hydrolytic activity of Zr<sup>IV</sup>-substituted Lindqvist-, Keggin-, and Wells–Dawson-type polyoxometalates towards the peptide bonds in tri- and tetrapeptides is investigated by kinetic methods and multinuclear NMR spectroscopy. The peptides are hydrolyzed completely in nearly neutral and neutral pH media. The Keggin complex is the most active towards peptide bond hydrolysis in the studied peptides.